ractor Report 2811

TECHNICAL
LIBRARY

Measurements of Blast Waves From Bursting Frangible Spheres Pressurized With Flash-Evaporating Vapor or Liquid

E. D. Esparza and W. E. Baker

DTIC QUALITY INSPECTED 4

NASA

NASA Contractor Report 2811

Measurements of Blast Waves From Bursting Frangible Spheres Pressurized With Flash-Evaporating Vapor or Liquid

E. D. Esparza and W. E. Baker
Southwest Research Institute
San Antonio, Texas

NASA

National Aeronautics
and Space Administration

**Scientific and Technical
Information Office**

1977

FOREWORD

The experiments reported here were funded by NASA Grant 3008, and conducted by Southwest Research Institute under subcontract to the University of Illinois. Several staff members at the Institute in addition to the authors contributed to the success of this investigation. The following are specially acknowledged:

- Messrs. E. R. Garcia and R. R. Hoffman for their assistance in conducting the experiments and recording the data

- Mses. P. A. Donovan and Y. Martinez for their help in the reduction and plotting of the data.

The helpful support, suggestions, and cooperation of Mr. Paul M. Ordin of the NASA Lewis Research Center and Prof. Roger A. Strehlow of the University of Illinois - UC are greatly appreciated.

TABLE OF CONTENTS

SUMMARY

The purposes of the experimental study reported here were to obtain basic data on blast waves generated by the bursting of frangible pressure vessels containing liquids under pressure which could flash evaporate during vessel burst, and to obtain blast data for frangible vessels which burst while containing dense gas under pressure. Side-on blast wave properties were to be measured for each of these blast sources at a number of radial distances.

The fluid chosen for the experiments was a common refrigerant, dichlorodifluoromethane (Freon ®-12), and the frangible spheres were made of blown glass. The spheres were fractured by impacting with a pneumatic striker while filled with either liquid or gaseous fluid under high pressure and room temperature. Blast parameters were measured using an array of side-on pressure transducers, connected to suitable amplifying and recording equipment. Measured parameters included positive and negative phase peak pressures, positive and negative phase impulses, times of first and second shock arrival, durations of positive and negative phases.

The bursting, liquid-filled spheres usually generated very low amplitude pressure waves which were essentially sound waves. The only exception was one test at the highest pressure ratio tested, and even this test produced only a weak blast wave. The vapor-filled spheres generated distinct blast waves in every test, with characteristics similar to those obtained with earlier tests of bursting spheres filled with air and argon. As was true for tests with air and argon, the blast wave characteristics differ from waves generated by condensed explosives in a number of respects. All data were scaled according to a blast scaling law developed earlier, and are presented in this form in the report. All reduced data for both liquid-filled and vapor-filled spheres are also presented in an appendix.

This is essentially a data report, containing what appears to be the first set of blast measurements for bursting frangible vessels filled with a flash-evaporating liquid or a dense gas. To supplement these data, other tests are suggested with heated flash-evaporating liquids. Supporting analyses are also suggested.

I. INTRODUCTION

As a continuation to experiments conducted with high-pressure air and argon frangible glass spheres simulating bursting of thin-walled gas pressure vessels [1], a set of similar experiments have been conducted using spheres of Freon(R)-12 (dichlorodifluoromethane) liquid and vapor. The objective of the experimental work reported here was to record time histories of side-on pressures at various distances from a blast source of flash-evaporating fluid.

The data obtained from the liquid tests showed much lower over-pressures than expected and, except for one experiment, the bursting of the pressurized liquid did not develop a shock front. However, the pressure records were similar for all measurement locations and from test to test.

On the other hand, the pressure-time traces for the vapor tests, in addition to being quite repeatable, were somewhat similar to those from the previously reported [1] air and argon experiments. The reduced data for blast overpressures, impulses, and other measured parameters are presented in dimensionless form and whenever possible compared to condensed explosive (Pentolite) data. In addition, this report describes the experiments and their setup. A discussion of the results follows, along with recommendations for future work.

II. THE EXPERIMENTS

A. General

There were twenty-one experiments conducted in this project, using glass spheres of two diameters and various thicknesses. Freon-12 was used in the liquid and vapor state to pressurize the 51 and 102 mm (2- and 4-in.) nominal diameter glass spheres. Room temperature liquid Freon-12 was used for eleven of the experiments, at gage pressures of 1,000 to 2,590 kPa (145 to 375 psig). The other ten experiments used vaporized Freon-12, also at room temperature, and internal pressures of 241 and 503 kPa (35 and 73 psig).

The experiments were conducted using the same experimental apparatus used by Esparza and Baker [1] in measuring overpressures from air and argon-pressurized frangible spheres. An array of eight side-on pressure transducers was used to record pressure-time histories at various distances along the radials from the glass spheres. As had been done in the previous investigation [1], high-speed cinematography was used in some of the tests to observe the sphere breakup and to obtain velocities of the glass fragments. Unfortunately, because of technical difficulties with the lighting system used, movie film data were obtained on only three experiments.

B. Experimental Layout

These tests were conducted in the same blast chamber at SwRI used in the previous work [1], as shown in Figure 1. The measuring equipment in the chamber included two aerodynamically-shaped, pencil-type blast pressure transducers and a double-wedge probe with six blast pressure transducers spaced along the upper surface. All eight of these transducers measured the side-on blast pressures generated by the bursting pressurized glass spheres. A high-speed camera, protected by a sheet of transparent plastic held in a wooden frame, photographed some of the events.

The glass spheres were blown from Pyrex glass tubing and were furnished with a neck about 51 mm (2-in.) long. Two different schemes were used to couple the spheres to the pressurization system. For all spheres, except the two used with the high-pressure liquid, a short piece of high-pressure nylon hose was used with hose clamps to connect the sphere to the steel tubing. For the other two spheres, the inside diameter of the neck of the spheres was 6.9 mm (0.25-in.) and a short piece of 6.35 mm (0.23-in.) steel tubing with a tube fitting was epoxied inside the neck to connect the spheres to the rest of the pressurization system.

Two different size glass spheres of 51 and 102 mm (2- and 4-in.) nominal diameter and several different thicknesses were hand blown for this project. The thickness of each sphere was selected so that the different internal pressures could be used to pressurize the spheres close to their break point. Therefore, a slight tap against the sphere would burst it relatively uniformly all around and create small-size fragments which would
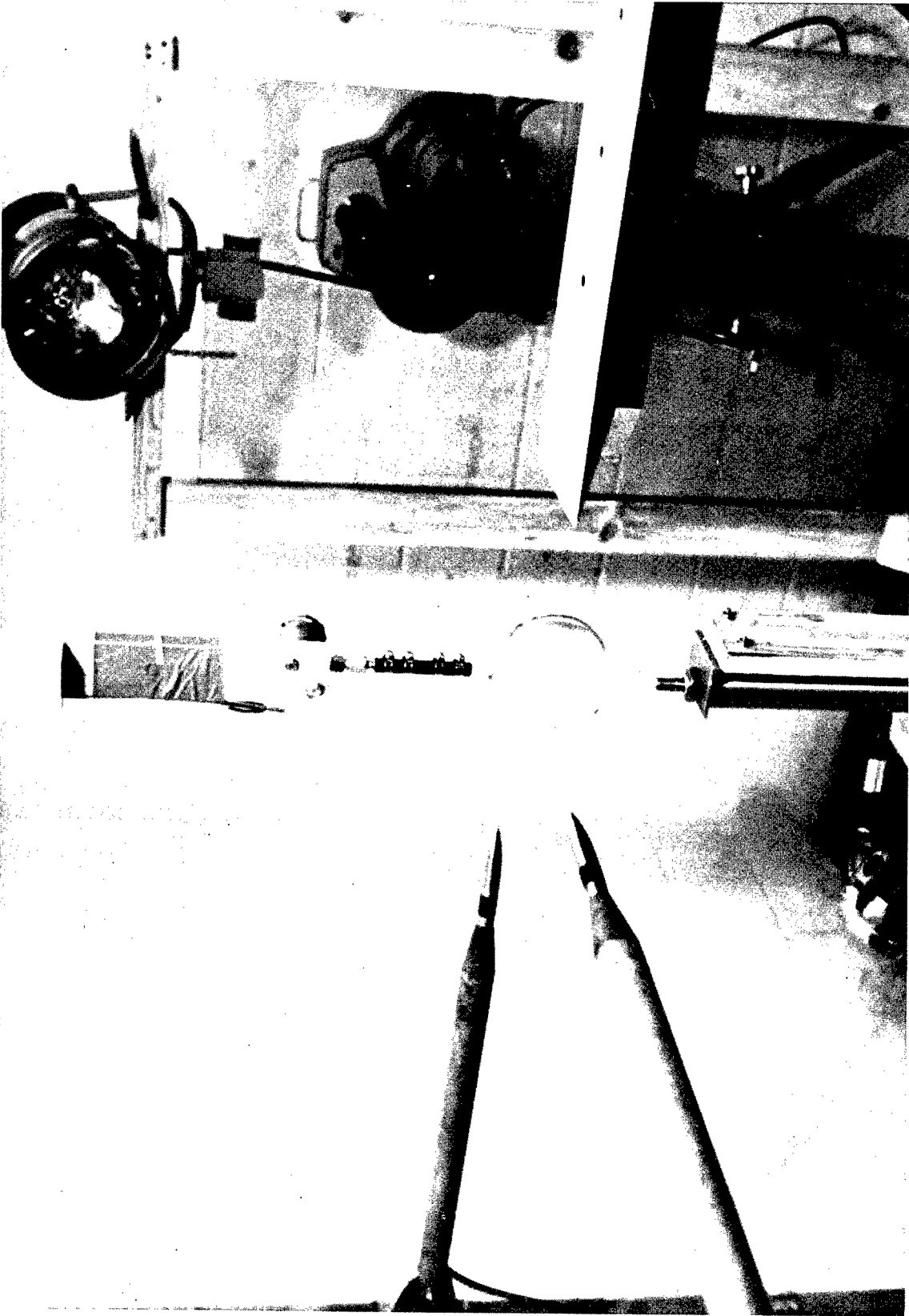
FIGURE 1. OVERVIEW OF EXPERIMENTAL APPARATUS

minimize the interference to the shock wave produced. The results in References 1 and 2 were used as a guideline for estimating the pressure which would burst each size sphere. However, nonuniformities in the spheres (particularly in the thicker and larger ones) caused the maximum pressure that spheres of the same size would withstand to vary. Consequently, several of the spheres burst prematurely on some tests, which precluded recording pressure data.

Because of the nonuniformity expected, each sphere tested was individually measured for mass, volume, and thickness. The sphere assembly was weighed before each test and the remains (usually the neck and its fittings) were weighed after each test to determine the total mass of the fragments. The volume was measured by filling the sphere with water up to the bottom of the neck and then emptying the contents into a graduate. Using this volume, a mean diameter was computed using the formula for the volume of a sphere. With this mean diameter and the measured mass of the sphere, a mean sphere thickness was also computed. The actual thickness was also measured using ultrasonic sensors by taking several spot measurements around the sphere and averaging the results. The spheres used ranged in thickness from 0.3 to 3.3 mm (0.012- to 0.13-in.). For the majority of the spheres, these average measured values were very close to the computed mean thickness.

C.   Test Procedure

A typical experimental test was conducted by first coupling a glass sphere to a remotely operated solenoid valve as shown in Figure 1. The solenoid valve was rigidly mounted onto wooden boards supported from the roof and was connected using steel tubing to the Freon-12 cylinders located in an adjacent test cell, as shown in the diagram on Figure 2. A precision bourdon-tube dial gage was used to monitor the pressure in the line (and in the sphere). Two manually operated valves, one adjacent to the solenoid valve and one near the Freon-12 cylinders, provided the means for venting line pressure, and for repeated purging of the sphere and tubing at low pressures using the vapor cylinder.

Once the sphere was properly connected to the solenoid valve and purged, a short length of very fine wire was lightly taped around the sphere for use in a break-circuit to provide a trigger voltage for the recording instrumentation. Then the pneumatic cylinder was positioned under the sphere so that, when pressurized, the striker would travel about 4 mm (0.16-in.) past the bottom surface of the sphere. The cylinder was mounted on a wooden table which provided vertical height adjustment for the different size spheres. The solenoid valve controlling the input to the pneumatic cylinder was connected to a normally open set of contacts in the high-speed camera which prevented the energizing of the solenoid by a 24-VDC supply until the camera was up to speed and ready to photograph the event. Checking to be sure that the camera contacts were in fact open and that the remote start switch for the camera was in the off position before opening the nitrogen bottle regulator connected to the pneumatic cylinder prevented any accidental breakage of the glass spheres.
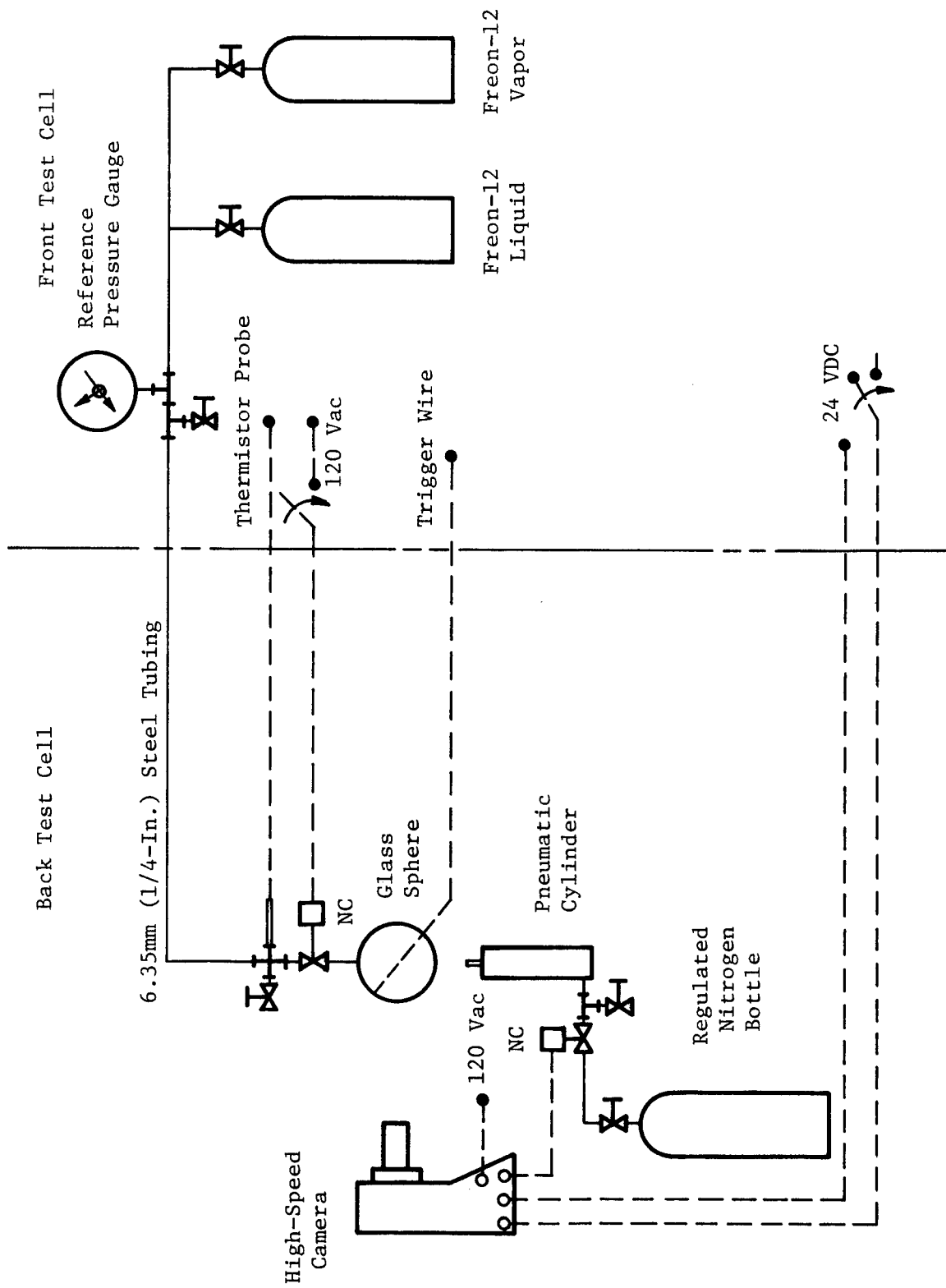
FIGURE 2. DIAGRAM OF EXPERIMENTAL SET-UP

The transducer holders were installed on vertical pipe stands so that vertical adjustment was possible. With the glass sphere already in place, the transducer probe point or edge was aligned along a radial through the sphere center. The three probes were placed 90° apart with the center probe opposite the movie camera. The tips of the other two probes were framed into the movie pictures to provide a known reference since the transducers were placed a measured distance from the exterior of the sphere. With the camera control connections verified to be in order, and the sphere and transducers properly installed, the camera was framed, focused, and loaded with a roll of high-speed negative film (Eastman 4x) and the camera speed set at a nominal 5000 frames per second. The back test cell was then evacuated and closed off.

The sphere was then pressurized using the appropriate source of Freon-12. The vapor source used was a commercially available cylinder whose gage pressure at 21.1°C (70°F) is 483 kPa (70 psig). The liquid Freon-12 was obtained by using a modified high-pressure cylinder so that 22.7 kg (50 lb$_m$) of Freon-12 was pressurized with nitrogen up to 3,448 kPa (500 psi) at room temperature. The pressurized liquid was drawn from the bottom of the cylinder with a "dip-tube" arrangement. The desired pressure was set by venting some of the nitrogen prior to opening the Freon-12 valve into the experimental setup. A thermistor temperature probe monitored the Freon-12 temperature as near the glass sphere as was physically possible. The remotely operated solenoid valve was kept open until the temperature in the line stabilized with ambient before it was closed in preparation for the test. In the case of the vapor experiments, this procedure took less than 10 minutes. In the case of the liquid experiments, the spheres filled up rather rapidly until the liquid level was about 3/4 full and then took much longer to fill the rest of the way, particularly for the larger volume spheres. By the time the spheres were full, the internal and ambient temperature had equalized. Once the temperatures were the same, the remotely controlled solenoid valve was deenergized (closed) and the tubing line partially vented. Enough positive pressure was kept so as to minimize the purging operation from test to test but low enough so that when the next sphere was used there was no danger of breaking it as the solenoid valve was again opened.

The high-speed camera and the spotlight were then turned on to begin the actual test. At a preset point of film travel, the contacts in the camera closed which energized the solenoid on the pneumatic cylinder. The cylinder was pressurized and the striker burst the sphere releasing the high-pressure contents. The bursting of the sphere broke the trigger wire which in turn triggered the pressure transducer's recording instrumentation. After the event, the high-speed camera was unloaded, the film processed, the pneumatic cylinder depressurized, the remains of the sphere removed and weighed, and the test cell cleaned and made ready for the next experiment.

D. Measurement System

The objective of this experimental effort was to obtain pressure-time records from free-field flash evaporating vapor and liquid explosions.

7

This was accomplished by using eight pressure transducers in a similar fashion as in Reference 1. The transducers used have minimum natural frequency of 67 kHz and are capable of accurately measuring overpressures down to 0.69 kPa (0.1 psi). The transducers were connected as shown in Figure 3 to SwRI-built impedance matching amplifiers consisting of a variable step capacitance input for different charge attenuation settings and into a field effect transistor circuit with very high input impedance. The output, which has a low impedance, was then slightly amplified for driving the cable lines to the data recorders. The frequency response of these units is about 0.1 Hz to 4 MHz. The outputs of the amplifiers were recorded on Polaroid film using a Biomation Model 802 digital recorder with Tektronix Model 602 display unit, a Tektronix Model R5444 dual beam oscilloscope with two Model 5A26 plug-in amplifiers, and two Tektronix Model R561B oscilloscopes with Model 3A75 plug-in amplifiers. The minimum recorded frequency response of any of these units as used was 250 kHz.

The reduced data obtained from these experiments included, whenever possible, the peak overpressures for both first and second shocks and their arrival times, first positive phase and negative phase impulses, and the durations of the first positive and negative phases. The data photographs were digitized, manipulated and plotted using a Hewlett-Packard Model 9830 microcomputer system. The pressure and impulse versus time plots were then used to read the various parameters of interest.
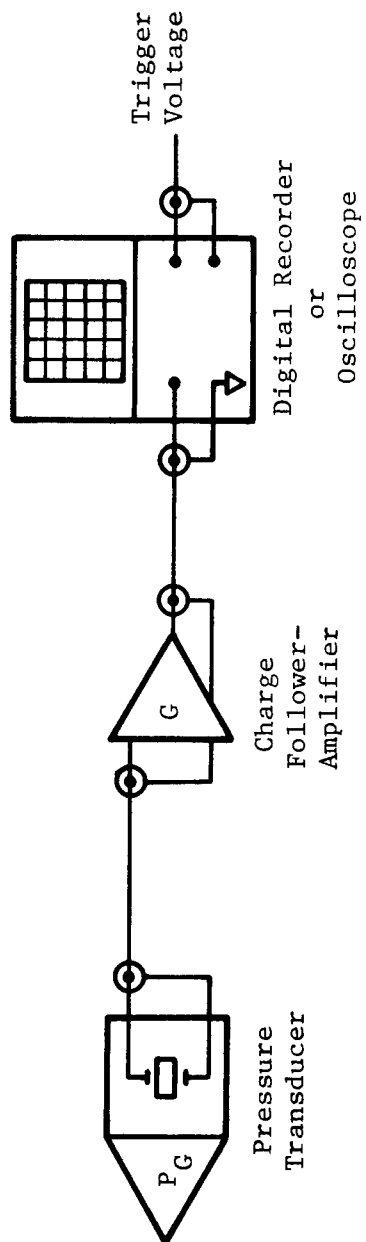
FIGURE 3. DIAGRAM OF PRESSURE MEASURING SYSTEM

III. RESULTS AND DISCUSSION

A. <u>General</u>

The data obtained in this experimental effort are presented in this section. All blast parameters plotted are nondimensional and are shown as functions of two non-dimensional variables $\bar{p}_1$ and $\bar{R}$ as follows:

$$
\left.
\begin{aligned}
\bar{P}_s &= \left(\frac{P_s}{P_a} \right) \\[2em]
\bar{t}_a &= \left(\frac{t_a a_a P_a^{1/3}}{E^{1/3}} \right) \\[2em]
\bar{T} &= \left(\frac{T a_a P_a^{1/3}}{E^{1/3}} \right) \\[2em]
\bar{I}_s &= \left(\frac{I_s a_a}{P_a^{2/3} E^{1/3}} \right)
\end{aligned}
\right\}
= f_i \left[\left(\frac{P_1}{P_a} \right) , \frac{R P_a^{1/3}}{E^{1/3}} \right]
\tag{1}
$$

where

P_a = amibent pressure (absolute)

a_a = ambient sound velocity

P_s = peak side-on overpressure

t_a = arrival time of the peak overpressure

T = duration of the overpressure

I_s = specific impulse

R = radius of blast wave (standoff distance)

P_1 = internal absolute pressure of sphere

10

E   = internal energy in the sphere

$$\overline{P}_1 = P_1/P_a$$

and

$$\overline{R} = \frac{Rp_a^{1/3}}{E^{1/3}}$$

The bars indicate non-dimensional quantities corresponding to the desired
dimensional quantities. This functional relationship is the reduced
form of the scaling law derived in Reference 1 for the formation and transmission
of blast waves from spheres of perfect gases with similar specific heat
ratios and sonic speeds. Because of the limited scope of the experimental
effort reported here, no analysis has been performed to develop a general
scaling law for flash-evaporating fluids. However, because only one fluid
has been used in this effort, it is very likely that the scaling law would
reduce to the relationship shown above such that the blast parameters are
primarily functions of $\overline{R}$ as was the case for the more perfect gases such
as air or argon [1], and only the overpressure showing some dependence on
$\overline{P}_1$.

Since all the nondimensional parameters, except two, contain the
internal energy in the sphere, E, a determination of this quantity is
required for computing the barred quantities. In Reference 1, the energy
in the sphere was computed using Huang and Chou's definition [4], which is
essentially the potential energy caused by the high pressure of the gas in the
sphere. For a perfect gas, the energy in the sphere given by this definition
is very close to what would be computed assuming the available energy
is that which is released by an isentropic expansion of the gas in the sphere
from a high pressure to an ambient pressure [5].

For a bursting sphere containing a flashing vapor or liquid such as
Freon-12, perfect gas behavior cannot be used to determine the energy of
the sphere. The maximum energy that can be released to drive a blast wave
can be estimated by assuming an isentropic expansion from the initial state
conditions to ambient pressure, and computing the corresponding work which
could be done as a change in internal energy of the expanding fluid. Similar
approximations have been used by other investigators to determine the energy
of an expansion pressure wave from a flash-evaporation process [6]. Based on
a unit mass of fluid, the energy change of a process starting at state 1 and
expanding to state 2 is

$$u_1 - u_2 = {_1}\!\int^2 p \, dv \qquad (2)$$

If the isentropic expansion process for Freon-12, which is usually a two-phase fluid, can be assumed to follow an expansion according to

$$p \, v^n = C \tag{3}$$

then Equation (2) gives

$$u_1 - u_2 = \frac{p_2 \, v_2 - p_1 \, v_1}{1 - n} \tag{4}$$

Two types of experiments were conducted with the Freon-12. In the first, liquid Freon filled the frangible spheres at pressures above saturation pressure for room temperature. In the second, room temperature saturated vapor or superheated vapor was used to fill the spheres. Tables of thermodynamic properties of Freon-12 are readily available. They give properties of saturated liquid, saturated vapor, and superheated vapor. No properties for compressed liquid seem to be available. (But, by analogy to properties of compressed water, very little internal energy can be stored in the compressed liquid, compared to a wet, dry or superheated vapor). Therefore, the first type of test, saturated liquid initial conditions were assumed to compute internal energy at state 1.

The procedure used to calculate maximum specific work, $u_1 - u_2$, is then to obtain values from tables for the initial conditions, including the entropy s_1 and enthalpy h_1. Compute u_1 from one of its definitions

$$u = h - pv \tag{5}$$

Assume expansion to a pressure in the table nearest to atmospheric, $p_2 \sim p_a$, with $s_2 = s_1$. Calculate quality x of vapor, if wet, from

$$x = \frac{s - s_f}{s_g - s_f} \tag{6}$$

Next, get

$$v_2 = v_f + x \, v_{fg} \tag{7}$$

and

$$h_2 = h_f + x \, h_{fg} \tag{8}$$

12

Use Equation (5) again for state 2 conditions to get u_2. If fluid in state 2 is in superheated region, u_2 is obtained from table values of h_2 and v_2. Finally, $u_1 - u_2$ is obtained, which is the desired result.

For a sphere of any given initial volume V_1, the mass of refrigerant can be calculated using V_1 and v_1 or its reciprocal γ_1. This mass is

$$m = V_1/v_1 \tag{9}$$

and the total energy input for the blast wave is

$$E = m \ (u_1 - u_2) \tag{10}$$

When the entire expansion process occurs in the superheated region, Equation (4) can be used to estimate the exponent n for isentropic expansion. Rearranged, this gives

$$n = \frac{p_1 \ v_1 - p_2 \ v_2}{u_1 - u_2} + 1 \tag{4a}$$

In this equation, n is the counterpart of γ for a perfect gas. Sample calculations for test conditions used in this program are given in Appendix A.

As in Reference 1, attempts were made to determine the kinetic energy of the glass fragments by the use of high-speed cinematography. Unfortunately, because of lighting difficulties, only three of the tests produced readable results for tests containing the refrigerant in vapor form. The films of the liquid tests showed that the glass pieces were projected at much lower velocities than those using vapor so that the expanding liquid quickly covered the fragments and then they became unobservable. However, even for the vapor spheres which had the higher fragment velocities and lower initial energy levels, the kinetic energy was at the most less than 10% of the isentropic change in internal energy. Furthermore, because the energy term always enters with an exponent of 1/3, not correcting for the kinetic energy of the fragments would result in a maximum error of 3% on the energy available for driving the blast wave.
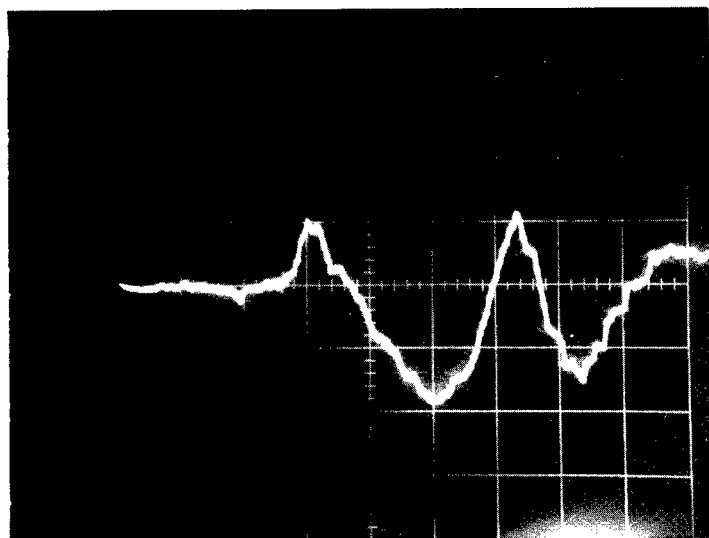
B. Liquid Spheres

There were eleven experiments attempted using Freon-12 at pressures well above the saturated vapor pressure at a room temperature of about 20°C (68°F). The compressed liquid filled the glass spheres completely at pressure ratios p_1/p_2 of 11.2 to 27.3. On three of the experiments, no data were obtained because the glass spheres burst prior to complete filling

with the liquid Freon-12. Because of the isentropic change in internal
energy which was available for driving the blast wave for these experiments
was comparable to the pressure energy used in the tests of Reference 1, the
recording instrumentation was set up to record voltage levels in the same
range as had been observed in the air and argon experiments. However, it
was soon evident after a couple of tests with liquid-filled spheres that, for
the range of scaled distances used, the peak overpressures were at least one
order of magnitude lower than expected. Consequently these two tests yielded
no recoverable data. Furthermore, it was evident that a shock front seldom
developed, except in one test which used one of the 102 mm spheres at the
highest pressure ratio used, p_1/p_a = 20.3, for this size sphere.
For this particular test, the overpressure at the closest measurement point,
$\bar{R}$ = 0.41, was only 5.9 kPa (0.86 psig). The rest of these tests yielded
even lower overpressures at the various measurement stations most of which
were lower than 1.4 kPa (0.2 psig). At these levels, the pressure transducers
used were close to their lower limit of measuring with acceptable accuracy
so that it was difficult to determine whether the scatter found in the data
was caused by inaccuracies in the measurement system or by the nature of the
experiment. Therefore, the data obtained have been presented only in
tabular form in Appendix B.

The general characteristic of the pressure-time histories recorded
for the liquid-filled sphere was as shown in Figure 4. A gradual positive
rise was followed by a long duration and larger amplitude negative phase.
A second, shorter duration positive phase then followed. In contrast,
Figure 5 shows that data recorded for Test No. 13 in which a shock front
similar to those recorded for the vapor (also for air and argon in Reference 1)
did develop. This figure is also an example of the reduced format of the
data used to obtain the various blast parameters.

Note that a shock developed only for the highest test pressure of the
largest sphere. The actual time scale for this test is, of course, considerably
longer than the time scales for tests for smaller spheres. We can speculate
that the liquid therefore had more time to evaporate and to generate a shock
wave in Test No. 13 than in any other test. But, we did not obtain enough
test data to be certain of this conclusion.

For these data, the first and second peak overpressures were obtained
as well as the positive and negative impulses. The rather low pressure
amplitudes recorded in view of the high energy available is probably due to
the relatively slow flash-evaporation of the liquid at the pressures used.
Thus not enough vapor was available at high pressure to develop a shock front.
Our high-speed films of these tests produced no data for fragment velocities,
but they did show that the liquid was dispersed at high velocity. All of
our blast transducers were side-on transducers oriented with sensing elements
parallel to the flow, and would therefore not measure dynamic or liquid
impact pressures. Again, we can speculate that dynamic pressures exerted on
objects immersed in the flow would be much higher than the side-on pressures,
but we do not know how much higher because we made no measurements.

14

Sensitivity: 0.86 kPa/div

$P_{s_1} = 0.92$ kPa, $R = 178$ mm

$\overline{P}_{s_1} = 0.0094$, $\overline{R} = 0.83$

Sweep: 1.0 ms/div

Test No. 14, Freon-12 Liquid
Sphere Diameter: 51 mm, $P_1/P_A = 11.2$
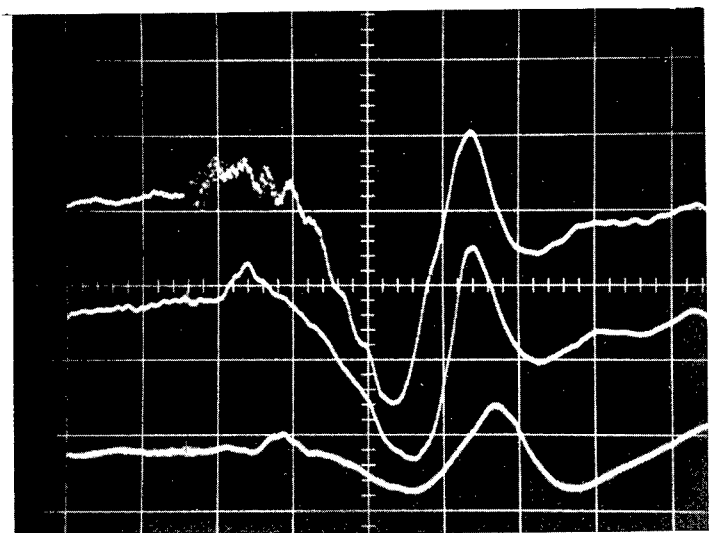
Upper Trace
   Sensitivity: 1.72 kPa/div

$\overline{P}_{s_1} = 0.0106$, $\overline{R} = 0.62$

Middle Trace
   Sensitivity: 1.59 kPa/div

$\overline{P}_{s_1} = 0.011$, $\overline{R} = 0.73$

Lower Trace
   Sensitivity: 2.41 kPa/div

$\overline{P}_{s_1} = 0.0068$, $\overline{R} = 1.23$

Sweep: 1.0 ms/div

Test No. 15, Freon-12 Liquid
Sphere Diameter: 51 mm, $P_1/P_A = 11.2$

Figure 4. Examples of Pressure-Time Histories From Bursting Spheres Pressurized with Liquid Freon-12

15
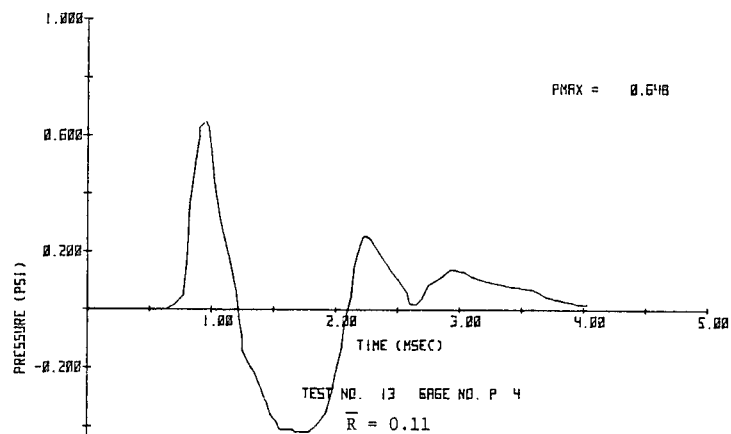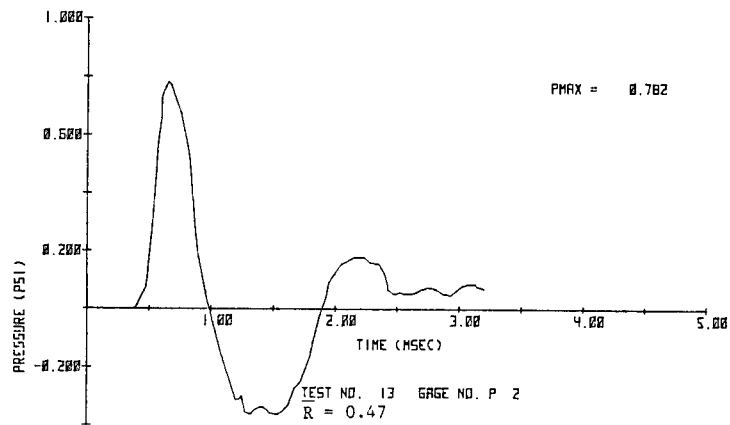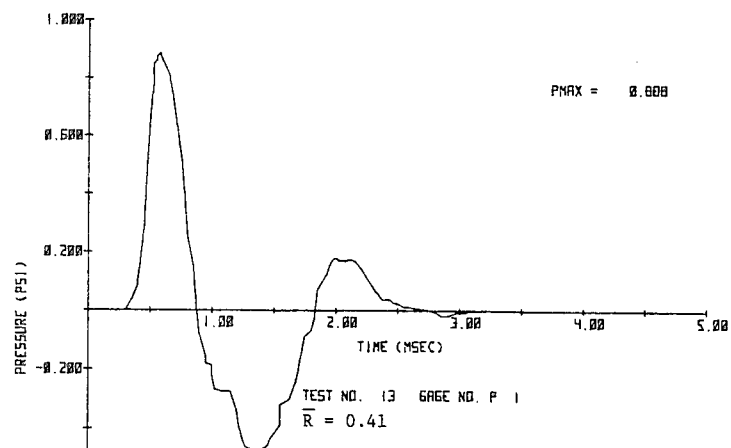
FIGURE 5. PRESSURE DATA FROM 102 MM LIQUID FREON-12 SPHERE
WITH $P_I/P_A = 20.3$

C. Vapor Spheres

There were ten experiments conducted using Freon-12 vapor in which blast data were obtained in every test. The pressure-time histories recorded were similar to those reported in Reference 1 for bursting spheres of air and argon. The traces were quite repeatable and are characterized by an initial shock overpressure, a gradual decay back to ambient, a significant negative pressure phase, and a second shock overpressure. The main differences in appearance between the data traces in Reference 1 and those recorded in this program are that the Freon-12 vapor traces have in general a relatively shorter negative phase duration and a higher second shock pressure compared to the first.* Figure 6 shows a number of examples of the Freon-12 vapor data recorded from both size spheres and internal pressures used in these tests. After digitizing and plotting the data from these types of records, the various blast parameters were read. The results were non-dimensionalized and are presented in graphical form in Figures 7 through 14. In these figures, two different size symbols are used to denote the two sphere sizes used in the experiments. Also, a differentiation is made in the symbols to show the two different internal vapor pressures used. In addition, whenever possible, the non-dimensional data are compared to data compiled for Pentolite high-explosive [3]. The scaled times of arrival of the first shock waves are presented in Figure 7. The $\bar{t}_{a_1}$ for bursting vapor spheres are comparable to those for a high-explosive over a decade of scaled distances $\bar{R}$ ranging from about 1.0 to 10.0. Note that the scaled times for the lower pressure experiments plot slightly lower than the rest, which indicates a slight dependence with initial internal pressure in the sphere. Also notice that scatter in the data increases with smaller values of $\bar{R}$. This is to be expected because of the poorer resolution, accuracy and repeatability of measuring shorter arrival times which use as a reference a trigger pulse from a break wire around the sphere.

In Figure 8, the peak side-on overpressure is shown as a function of $\bar{R}$. These data do not group together as closely as the time of arrival data. Some differences are evident between the small and large sphere data for a pressure ratio $\bar{p}_1 = 6$, and between these two sets of data and the large sphere data for $\bar{p}_1 = 3.5$. These differences indicate that, in addition to the dependence on $\bar{R}$ and $\bar{p}_1$, the side-on overpressure must also depend on other parameters for proper scaling. As shown, however, all the data are of lower amplitude than data from the high-explosive.

The scaled duration data of the first positive overpressures are shown in Figure 9 and are compared to the Pentolite curve. The data seem to group together by value of $\bar{p}_1$, and for $\bar{p}_1 = 6$ the two different size spheres experiments yield analogous results. The positive scaled time durations appear relatively constant for the range of $\bar{R}$ tested such that $\bar{T}_{s_1}$ (+) has

---

* The scaled durations for Freon-12 vapor are considerably longer than scaled durations for air or argon, for equal scaled distances.
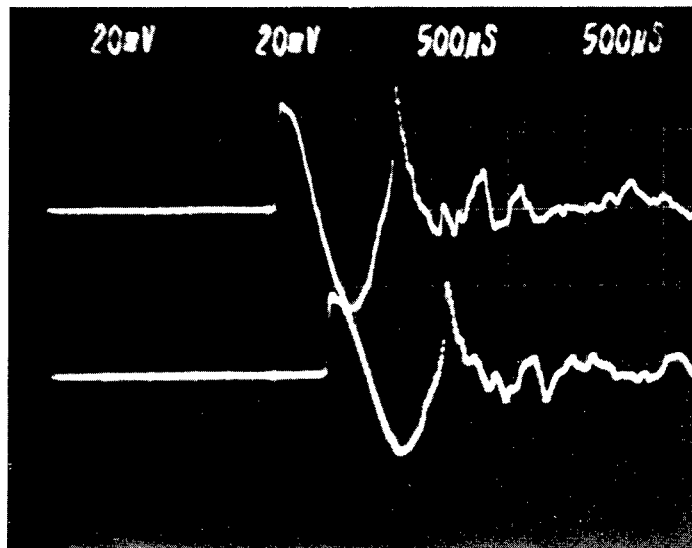
Upper Trace
   Sensitivity: 1.03 kPa/div
   P_{s_1} = 1.45 kPa, R = 584 mm
   $\overline{P}_{s_1}$ = 0.015, $\overline{R}$ = 6.81

Lower Trace
   Sensitivity: 1.03 kPa/div
   P_{s_1} = 1.1 kPa, R = 686 mm
   $\overline{P}_{s_1}$ = 0.011, $\overline{R}$ = 8.00

Sweep: 500 ms/div

TEST NO. 16, FREON-12 VAPOR
SPHERE DIAMETER = 51 MM, P_1/P_A = 6
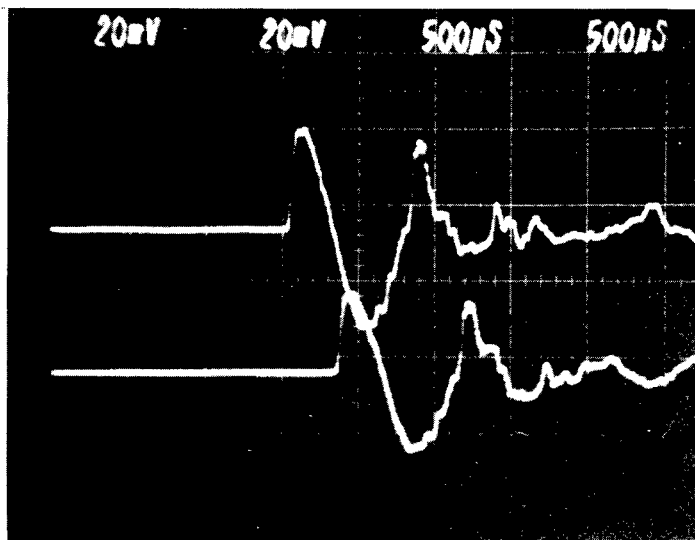
Upper Trace
   Sensitivity: 1.03 kPa/div
   P_{s_1} = 1.31 kPa, R = 584 mm
   $\overline{P}_{s_1}$ = 0.013, $\overline{R}$ = 6.68

Lower Trace
   Sensitivity: 1.03 kPa/div
   P_{s_1} = 1.03 kPa, R = 686 mm
   $\overline{P}_{s_1}$ = 0.011, $\overline{R}$ = 7.84

Sweep: 500 ms/div

TEST NO. 17, FREON-12 VAPOR
SPHERE DIAMETER = 51 MM, P_1/P_A = 6

FIGURE 6. EXAMPLES OF PRESSURE-TIME HISTORIES FROM
              BURSTING SPHERES PRESSURIZED WITH FREON-12 VAPOR

18
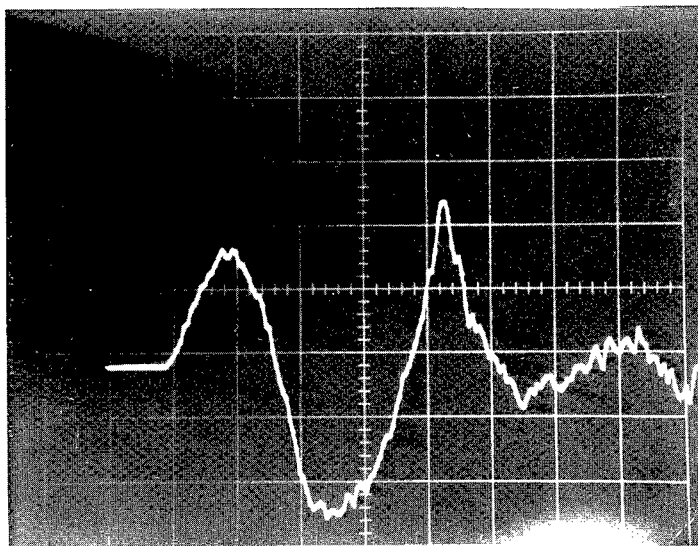
Sensitivity: 1.72 kPa/div

P_{s_1} = 3.24 kPa, R = 203 mm

$\overline{P}_{s_1}$ = 0.033, $\overline{R}$ = 1.54

Sweep: 400 ms/div

TEST NO. 21, FREON-12 VAPOR
SPHERE DIAMETER = 102 MM, P_1/P_A = 3.5
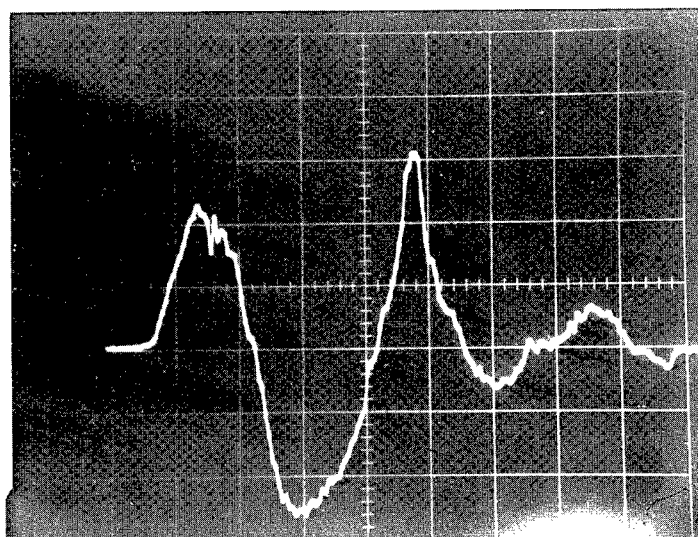
Sensitivity: 1.72 kPa/div

P_{s_1} = 3.93 kPa, R = 203 mm

$\overline{P}_{s_1}$ = 0.04, $\overline{R}$ = 1.60

Sweep: 400 ms/div

TEST NO. 20, FREON-12 VAPOR
SPHERE DIAMETER = 102 MM, P_1/P_A = 3.5

FIGURE 6. EXAMPLES OF PRESSURE-TIME HISTORIES FROM BURSTING
SPHERES PRESSURIZED WITH FREON-12 VAPOR (CONT'D)
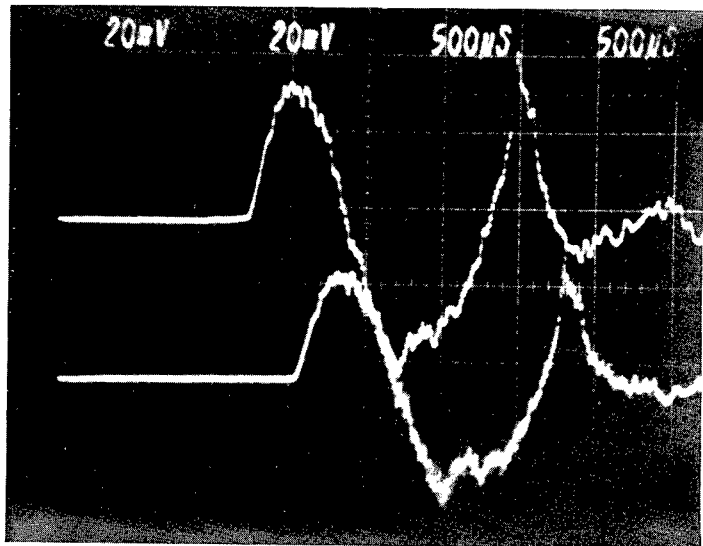
Upper Trace
Sensitivity: 1.03 kPa/div
P_{s_1} = 1.86 kPa, R = 610 mm

$\overline{P}_{s_1}$ = 0.019, $\overline{R}$ = 3.73

Lower Trace
Sensitivity: 1.03 kPa/div
P_{s_1} = 1.52 kPa, R = 711 mm

$\overline{P}_{s_1}$ = 0.015, $\overline{R}$ = 4.35

Sweep: 500 ms/div

TEST NO. 19, FREON-12 VAPOR
SPHERE DIAMETER = 102 MM, P_1/P_A = 6
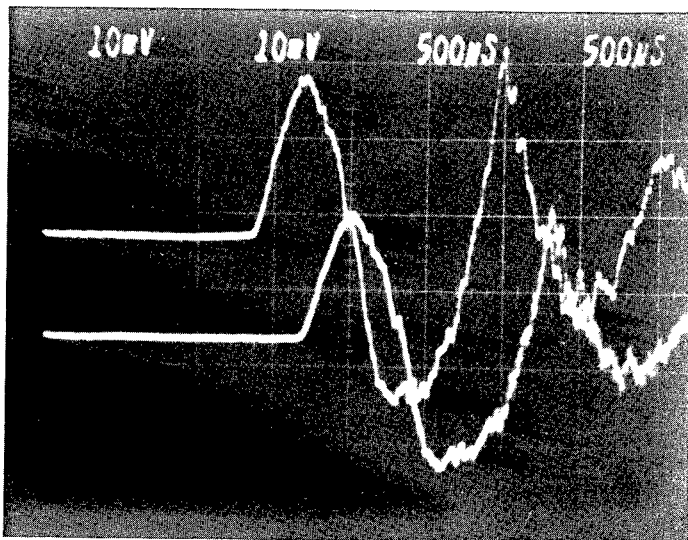
Upper Trace
Sensitivity: 0.52 kPa/div
P_{s_1} = 1.1 kPa, R = 610 mm

$\overline{P}_{s_1}$ = 0.011, $\overline{R}$ = 4.62

Lower Trace
Sensitivity: 0.52 kPa/div
P_{s_1} = 0.83 kPa, R = 711 mm

$\overline{P}_{s_1}$ = 0.0084, $\overline{R}$ = 5.39

Sweep: 500 ms/div

TEST NO. 21, FREON-12 VAPOR
SPHERE DIAMETER = 102 MM, P_1/P_A = 3.5

FIGURE 6. EXAMPLES OF PRESSURE-TIME HISTORIES FROM BURSTING
SPHERES PRESSURIZED WITH FREON-12 VAPOR (CONT'D)

20

FIGURE 7. SCALED TIME OF ARRIVAL OF FIRST SHOCK WAVE FROM BURSTING FREON-12 VAPOR SPHERE AT ROOM TEMPERATURE

21
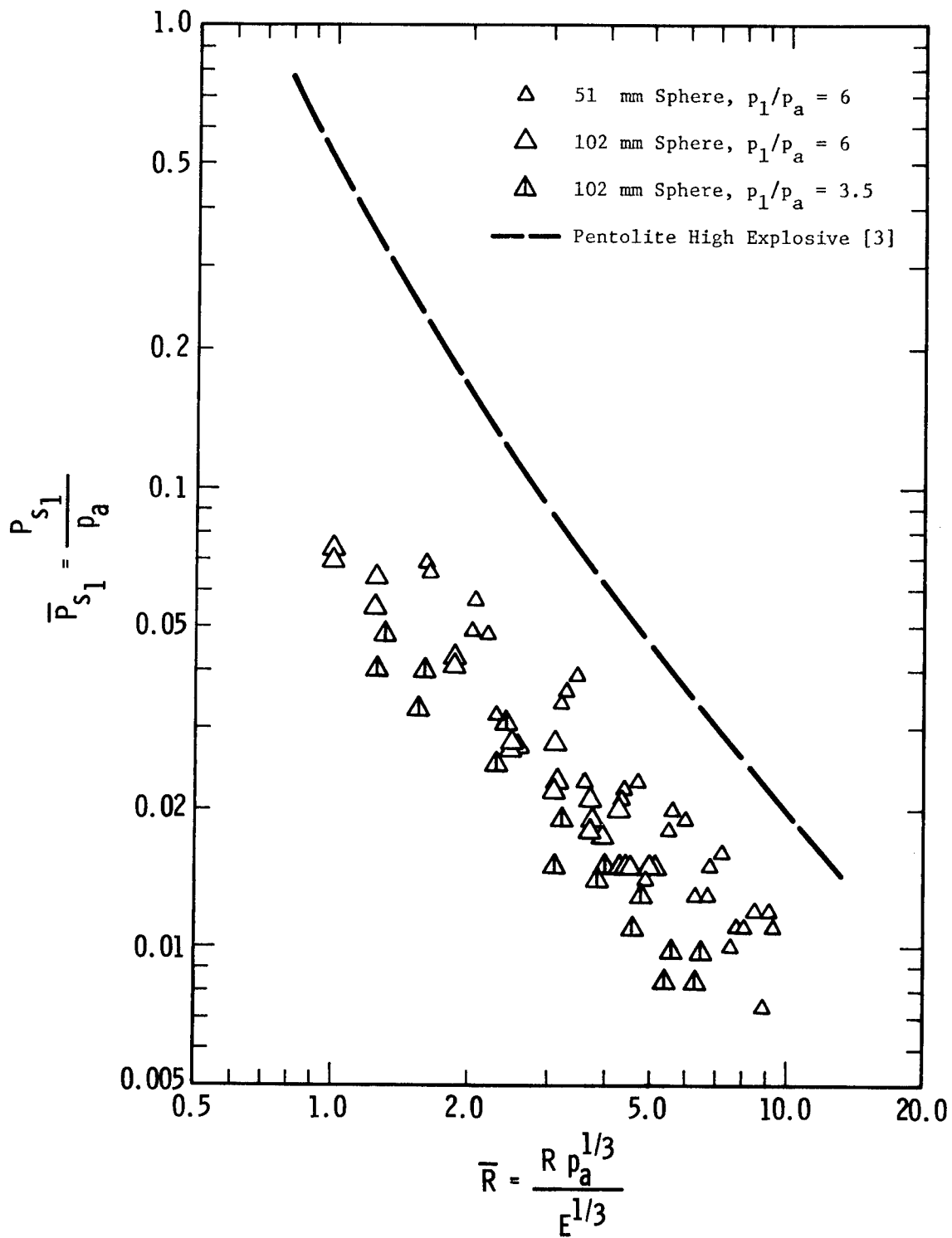
FIGURE 8. SCALED SIDE-ON PEAK OVERPRESSURE FOR BURSTING
FREON-12 VAPOR SPHERE AT ROOM TEMPERATURE
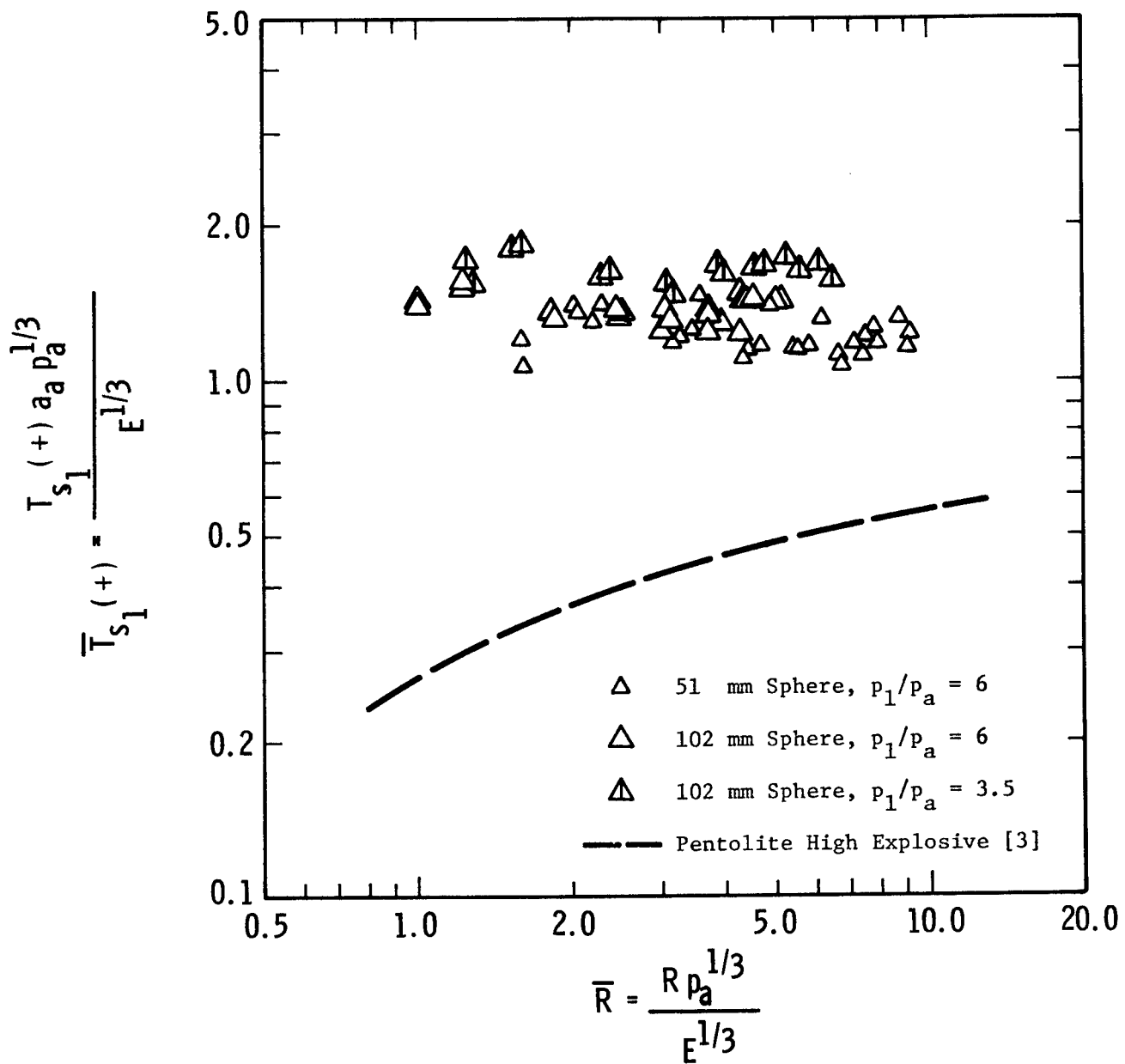
FIGURE 9. SCALED DURATION OF POSITIVE PHASE OF BLAST WAVE
FROM BURSTING FREON-12 VAPOR SPHERE

a mean value of almost 1.4. This value is about 2.5 to 5 times longer than the scaled durations for the Pentolite over the tested scaled distances.

The values of $\bar{P}_{s_1}$ measured for these experiments were lower than those of Pentolite. The magnitudes of $\bar{T}_{s_1}$ (+) were higher. However, the scaled side-on positive impulses measured which are interdependent with these two blast parameters compare closely to the high-explosive values. This is shown in Figure 10. The data points group together rather well with a slight tendency for the smaller sphere tests to yield slightly higher scaled impulses than the larger sphere tests.

The negative phase duration and impulse data are presented in Figures 11 and 12, respectively. Similar dependence on $\bar{R}$ can be seen for these negative phase parameters as was observed for the corresponding positive phase data. In this case, the scaled durations appear to be constant regardless of scaled distance used. The mean value of $\bar{T}_s$ (−) is about 1.9 and, as a result, the negative impulses are slightly higher than the positive impulses at corresponding scaled distances.

Finally, the scaled time of arrival and peak overpressure data from the second shock wave are shown in Figures 13 and 14. The time of arrival data points group together quite well, while the overpressure seems to scatter more and separate slightly for the two different values of $\bar{p}_1$ used. This is similar to the way the data behaved for the first shock wave. The overpressure amplitudes for the second shock front are slightly higher than for the first.

24
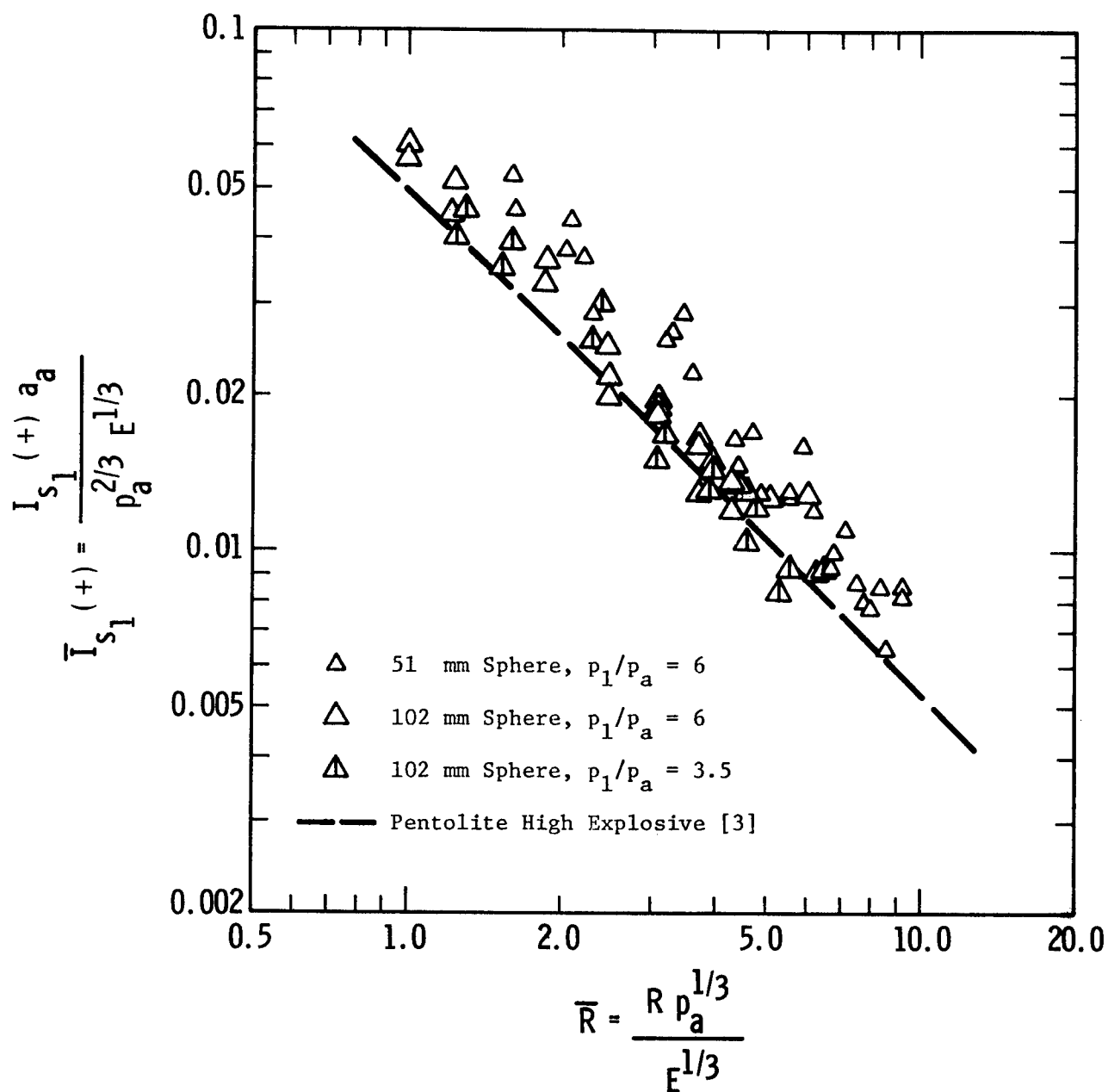
FIGURE 10.   SCALED SIDE-ON POSITIVE IMPULSE FROM BURSTING
FREON-12 VAPOR SPHERE

FIGURE 11. SCALED DURATION OF NEGATIVE PHASE OF BLAST WAVE
FROM BURSTING FREON-12 VAPOR SPHERE

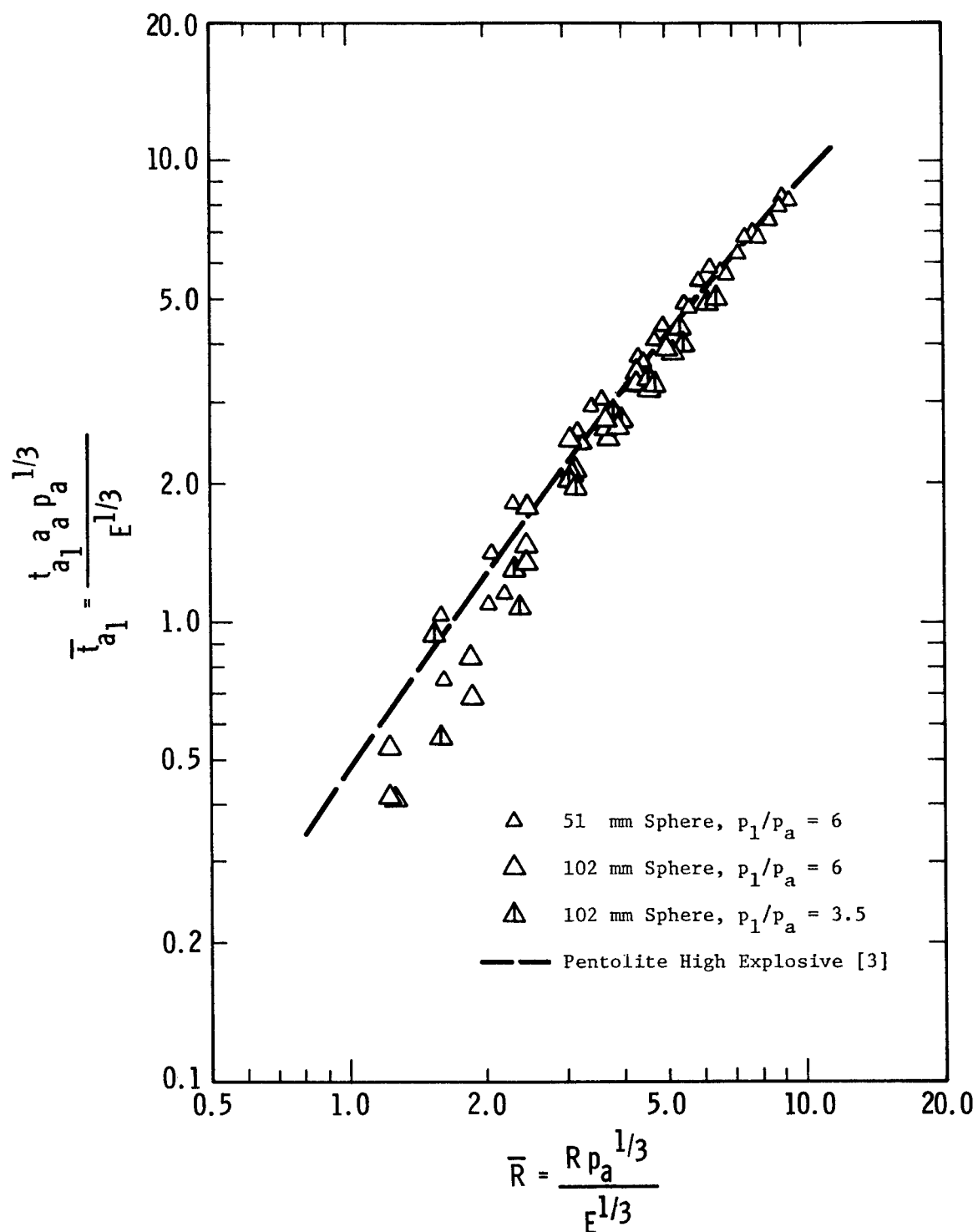FIGURE 12. SCALED SIDE-ON NEGATIVE IMPULSE FROM
BURSTING FREON-12 VAPOR SPHERE

FIGURE 13. SCALED TIME OF ARRIVAL OF SECOND SHOCK WAVE
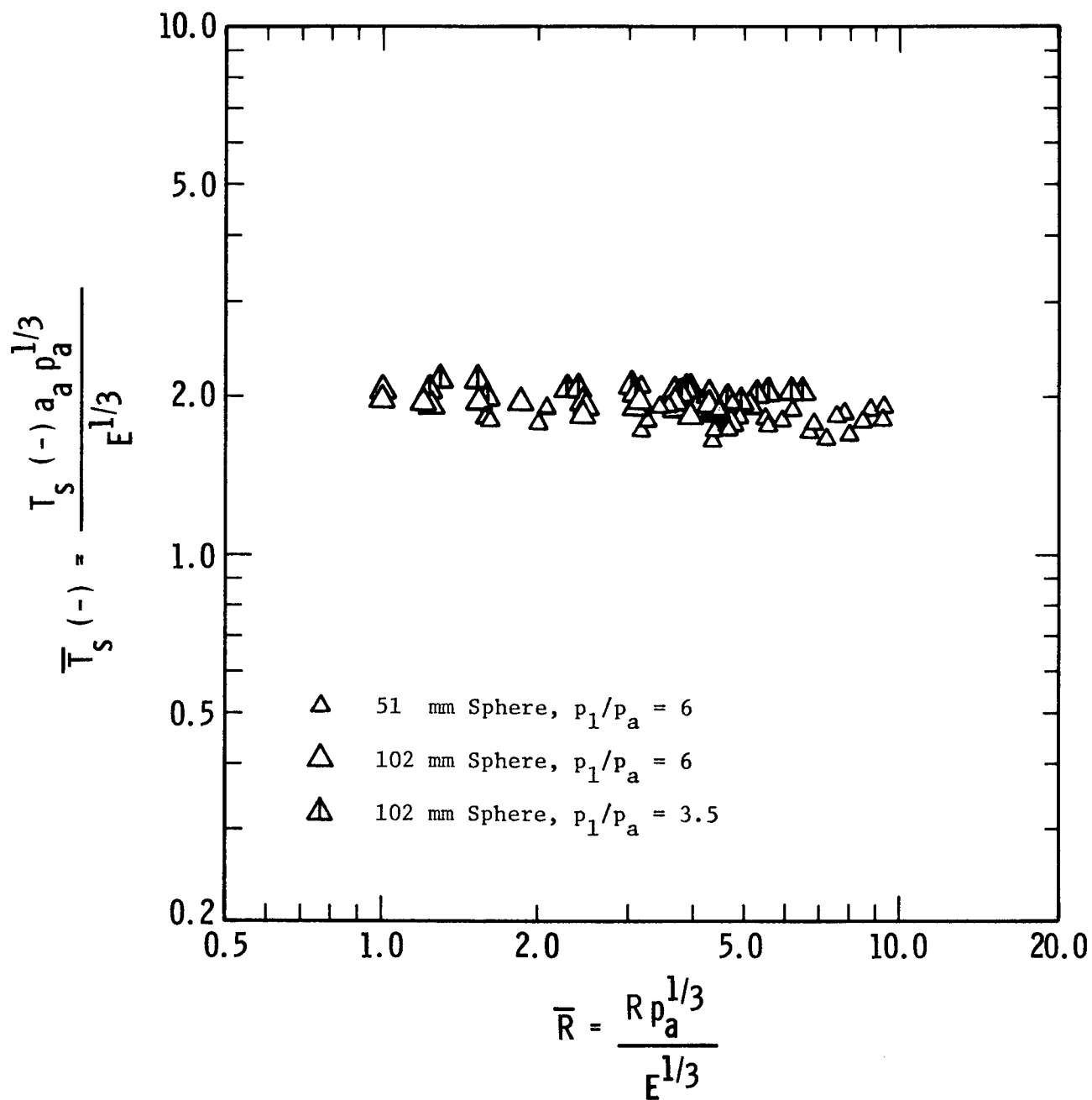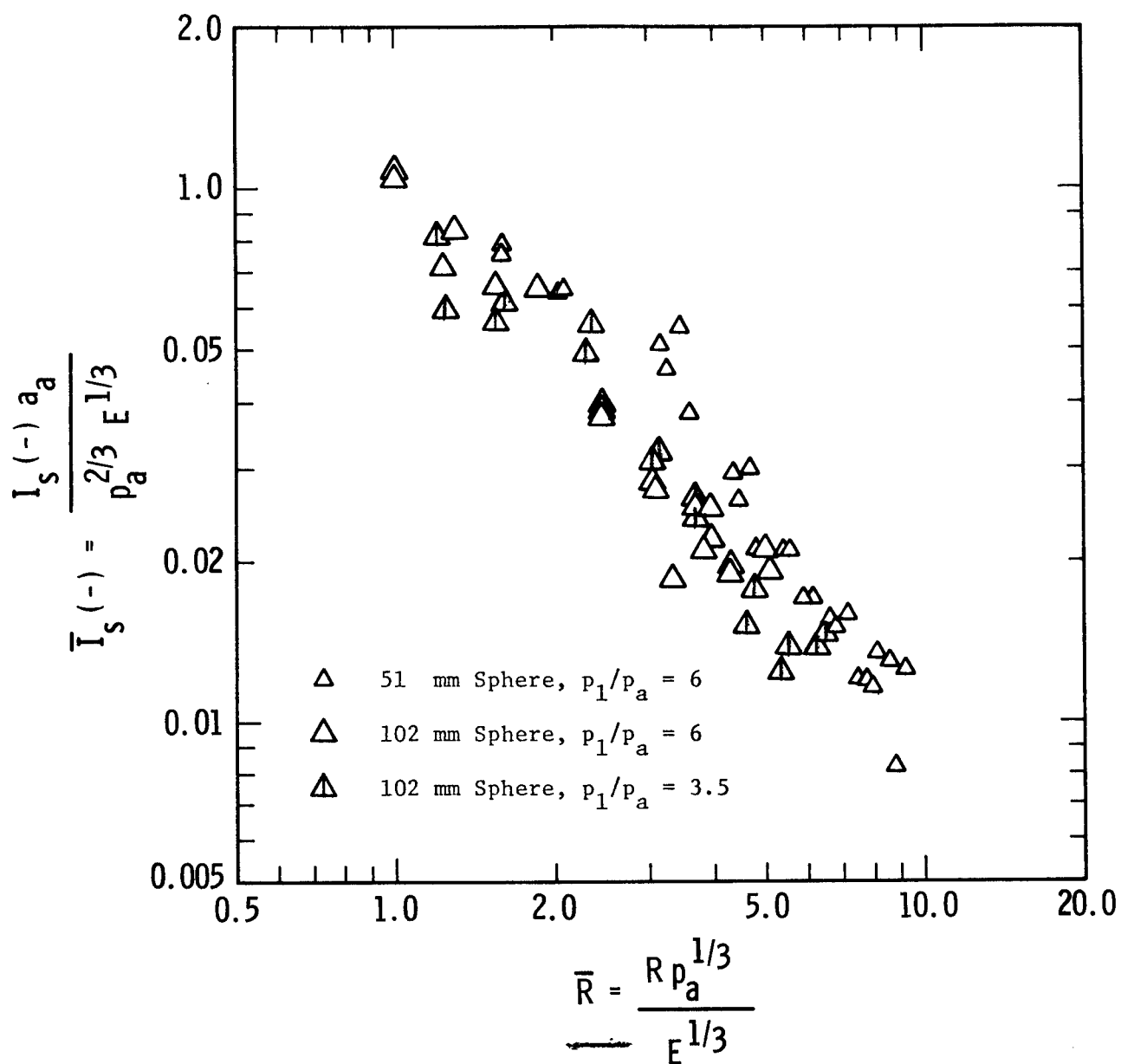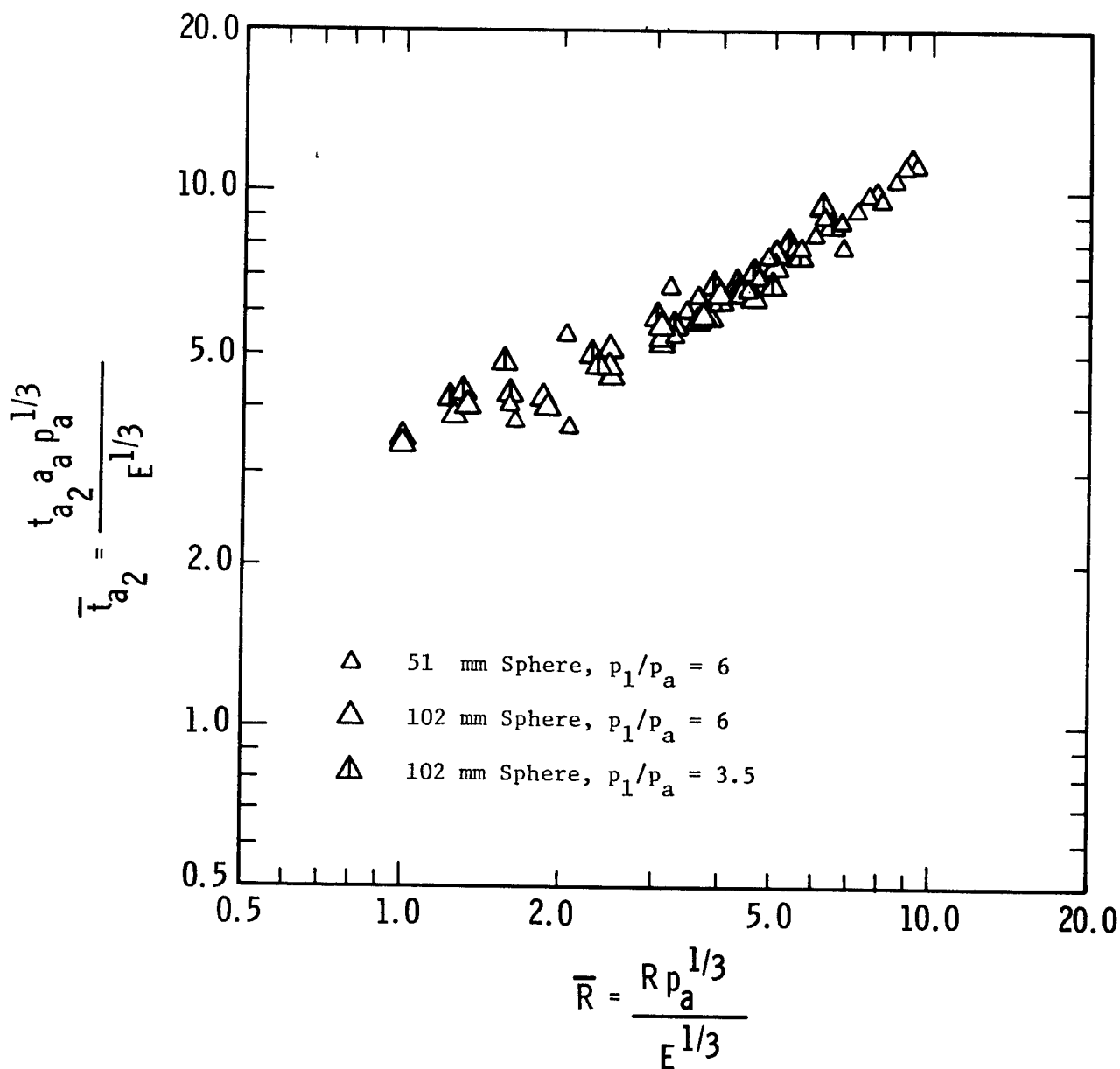FROM BURSTING FREON-12 VAPOR SPHERE
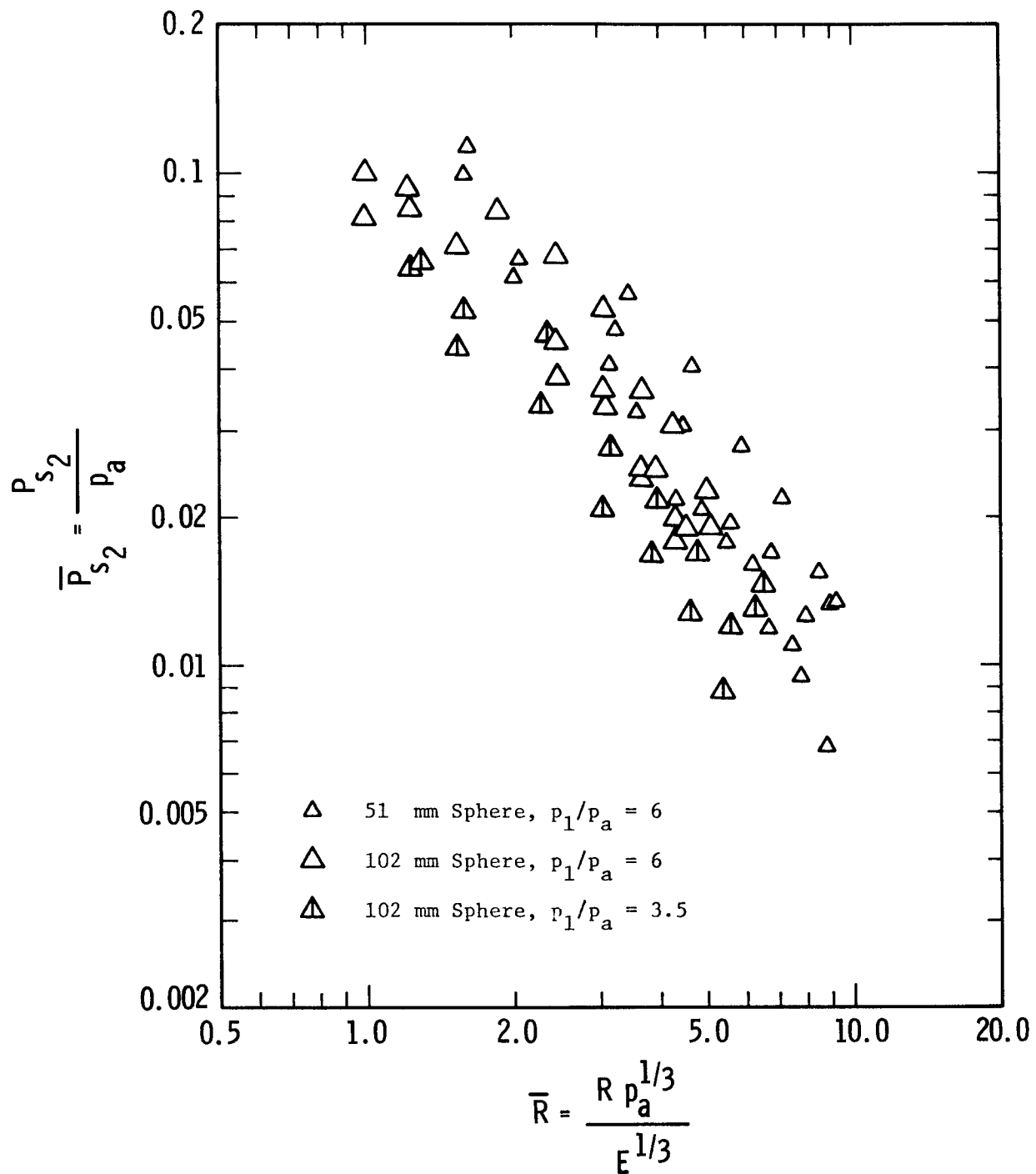
FIGURE 14. SCALED SIDE-ON PEAK OVERPRESSURE OF SECOND SHOCK
WAVE FROM BURSTING FREON-12 VAPOR SPHERE

IV. CONCLUSIONS AND RECOMMENDATIONS

Small-scale experiments were conducted by Southwest Research Institute to produce data on incident overpressures at various distances from frangible spheres pressurized with Freon-12 liquid and vapor. Since no quantitative data from this type of experiment are available in the literature, complete time histories of overpressure were obtained using an array of side-on pressure transducers to characterize the blast waves formed by the bursting glass spheres containing a flash-evaporating liquid or vapor. Two different size spheres were used of nominal diameters of 51 and 102 mm (2 and 4 in.)

The liquid experiments generated overpressures which were considerably lower in amplitude than expected for the energy available, assuming an isentropic expansion. Consequently, most of the measurements made were of lower amplitude than the low end of the pressure range over which the pressure transducer will measure with accuracy. Therefore, it is difficult to establish whether the large scatter in the data was a result of this problem and/or just the nature of the experiment. For this reason, and because only one of these experiments actually resulted in a shock propagation, only pressure and impulse data were reduced for the first two waves, and have been presented solely in tabular form.

The recorded blast waves for the vapor experiments were quite repeatable and somewhat different in appearance and relative amplitudes from waves produced by similar experiments using high-pressure air and argon spheres or condensed explosives such as Pentolite. The initial positive phase was followed by a very pronounced negative phase and a large amplitude second shock.

The results of the vapor tests in this limited experimental effort were transformed into non-dimensional quantities and plotted versus a scaled distance which corresponded to the various distances from the spheres at which pressure transducers were positioned. Whenever possible, these data were compared with compiled data for Pentolite high-explosive. Most of the blast parameters from the non-ideal explosions used in this work depend primarily on the scaled distance although some dependence in some of the parameters is evident for change in initial internal pressure in the sphere or the physical size of the energy source. Reduced data from these experiments include the peak overpressures and arrival times of the first and second shock, durations of the first positive phase and negative phase, and the positive and negative phase impulses.

These data appear to be the first set of measurements of the characteristics of blast waves from bursting, frangible spheres pressurized with a flash-evaporating fluid. However, since this set of experiments used only one fluid, additional experiments using the basic test arrangement and methods reported here are recommended to supplement these data. These experiments should include:

(1) Tests of bursting spheres filled with vapors of higher saturation pressure such as Freon-22, Freon-13, or sulfur hexafluoride (SF_6) to better determine the effect of sphere pressure on the overpressures measured.

30

(2)   Tests using the same fluids as above but in liquid form just above saturation pressure at room temperature.

(3)   Tests using flash-evaporating fluids in liquid form at a high-pressure heated above room temperature to just below the saturation temperature.

A last recommendation is to look, through a model analysis, at what form the scaling law for blast waves from flash-evaporating fluid spheres should take to better present the non-dimensional parameters. At the same time, the methodology for computing the energy for driving the blast waves which account for the fragmentation of the glass sphere needs to be analyzed to better apply the scaling law and to accurately compute the non-dimensional blast parameters for comparison with high-explosive data or analytic predictions. Thus, better risk assessments and damage predictions from accidental explosion of pressure vessels containing flash-evaporating fluids could be made.

APPENDIX A

SAMPLE ENERGY CALCULATIONS

The following sample calculations use English units of measure because tables of thermodynamic properties for Freon-12 are readily available only in this system of units [7].

Isentropic expansion of Freon-12 liquid at $p_1/p_a = 20.3$ and room temperature $\theta = 76°F$. Since no properties for compressed (subcooled) liquid Freon-12 seem to be available, properties for state 1 will be assumed as those of a saturated liquid. Furthermore, since this is an estimate of the change in internal energy caused by the expansion of the pressurized refrigerant, interpolation of table values will be minimized.

For $p_1 = 290$ psia ~ 296 psia

specific volume $v_1 = 0.01465$ ft^3/lb$_m$

enthalpy $h_1 = 48.065$ Btu/lb$_m$

entropy $s_1 = 0.091159$ Btu/lb$_m$°F

and internal energy $u_1 = h_1 - p_1 v_1$,

therefore $u_1 = 47.27$ Btu/lb$_m$.

At state 2 after expansion $(s_1 = s_2)$ to $p_2 \sim 14.22$ psia, the quality of vapor x is

$$x = \frac{s_1 - s_f}{s_g - s_f} = 0.508$$

where subscript f means fluid and subscript g means gas.

Therefore,

$$v_2 = v_f + x \, v_{fg} = 1.328 \text{ ft}^3/\text{lb}_m$$

$$h_2 = h_f + x \, h_{fg} = 39.759 \text{ Btu/lb}_m$$

and

$$u_2 = h_2 - p_2 v_2 = 36.263 \text{ Btu/lb}_m$$

Thus,

$$u_1 - u_2 = 11.0 \text{ Btu/lb}_m$$

Converting this to an energy per unit volume,

$$\frac{\Delta u}{v_1} = 247.6 \text{ Btu/ft}^3$$

For Test No. 13, the estimated energy available due to an isentropic expansion was

$$E = 247.6 \text{ V} = 127,000 \text{ in-lb}_f$$

or

$$E = 14,300 \text{ Joules}$$

If the fragment velocity is measured , then the kinetic energy of the fragments would be subtracted to obtain the energy available for driving a blast wave.

For an isentropic expansion of Freon-12 vapor at p_1/p_a = 3.45 and θ_1 = 78°F,

$$v_1 = 0.90 \text{ ft}^3/\text{lb}_m$$

$$h_1 = 88.42 \text{ Btu/lb}_m$$

$$s_1 = 0.17984 \text{ Btu/lb}_m - °F$$

and

$$u_1 = h_1 - p_1 v_1 = 80.2 \ \text{Btu/lb}_m$$

At $p_2 \sim 14.0$ psia

$$s_2 = s_1 > s_g \quad \text{(still in superheated region)}$$

$$v_2 = 2.83 \ \text{ft}^3/\text{lb}_m$$

$$h_2 = 78.42 \ \text{Btu/lb}_m$$

and

$$u_2 = 71.09 \ \text{Btu/lb}_m$$

Therefore,

$$\Delta u = 9.11 \ \text{Btu/lb}_m$$

and

$$\frac{\Delta u}{v_1} = 3.337V$$

For Test No. 21,

$$E - 3.337 \, V = 2,056 \, \text{in-lb}_f$$

or

$$E = 232 \, \text{Joules}$$

APPENDIX B

DATA TABLES

The non-dimensional data obtained in this program, along with the glass sphere characteristics for each test, are presented in this Appendix. Most of the column headings are self-explanatory; however, a short explanation of each follows:

. Internal Pressure - the absolute pressure used in the sphere ratioed to the ambient pressure

. Volume - the actual volume measured for each sphere.

. Computed Diameter - the diameter of the sphere as computed from the measured volume.

. Mass - the mass of the glass sphere obtained by taking the difference of the total mass of the sphere assembly before the test and the mass of the remains on the test fixture after the test.

. Thickness - computed from the measured mass and diameter of the sphere, and specific gravity of the glass.

. Energy - the estimated energy available for driving the blast wave assuming an isentropic expansion and very little fragment kinetic energy loss. Sample computations are given in Appendix A.

. All non-dimensional parameters used have been defined in Section III. The local atmospheric constants used in some of these parameters were:

$$P_a = 98.5 \text{ kPa} = 14.3 \text{ psi}$$

$$a_a = 339.3 \text{ m/s} = 13,360 \text{ in./sec}$$

36

Table B-1

Freon-12 Liquid Bursting Sphere Data

Test No.	Internal Pressure (p_1/p_a)	Volume (cm^3)	Computed Diameter (mm)	Mass (gm)	Computed Thickness (mm)	Energy E (Joules)	$\bar{R}$	$\bar{P}_{s_1}$	$\bar{I}_{s_1}(+)$	$\bar{I}_s(-)$	$\bar{P}_{s_2}$
2	11.9	480	97.1	137.2	2.0	7,560	0.72	0.0065	0.0017		
							0.96	0.0050	0.0017		
							1.43	0.0031	0.0011		
							1.67	0.0014	0.0011		
10	23.4	57	47.7	35.3	2.1	1,729	0.54	0.0074	0.00816	0.00620	0.0076
							0.64	0.0060	0.0102	0.0335	0.0068
							1.07	0.0010	0.00218	0.00281	0.0033
							1.47	0.0027	0.00444	0.00805	0.0065
							1.86	0.0032	0.00528	0.00802	0.0042
							2.25	0.0027	0.00498	0.00526	0.0038
							2.64	0.0019	0.00353		0.0031
11	23.4	59	48.3	39.7	2.3	1,729	0.53	0.0200	0.0266	0.0811	0.0278
							0.63	0.0173	0.0236	--	--
							0.68	0.0100	0.0155	--	--
							1.06	0.00506	0.00833	0.0191	0.0227
13	20.3	512	99.2	234.8	3.3	14,300	0.36	0.0600	0.013	0.011	0.013
							0.42	0.0556	0.011	0.011	0.013
							0.71	0.0472	0.0077	0.012	0.020
14	10.2	63	49.4	13.1	0.7	983	0.65	0.0124	0.0132	0.0757	0.0100
							0.77	0.00980	0.0109	0.0507	0.00614
							0.83	0.00938	0.00611	0.0350	0.0101
							1.30	0.00685	0.00791	0.0151	0.0108
							1.77	0.00390	0.00594	0.0110	0.00546
							2.24	0.00361	0.00577	0.00947	0.00441
							2.71	0.00308	0.00693	0.00798	0.00266
							3.18	0.00266	0.00598	0.00632	0.00252
15	10.2	73	51.9	12.8	0.7	1,141	0.62	0.0106	0.0168	0.0733	0.0162
							0.73	0.0110	0.0166	0.0539	0.0141
							0.79	0.0116	0.0168	0.0411	0.0148
							1.23	0.00679	0.00800	0.0187	0.0149
							1.68	0.00458	0.00523	0.0129	0.00826
							2.13	0.00480	0.00769	0.0110	0.00644
							2.58	0.00384	0.00717	0.0102	0.00483
							3.03	0.00314	0.00582	0.00747	0.00378

Table B-2

Freon-12 Vapor Bursting Sphere Data

Test No.	Internal Pressure (p_1/p_a)	Volume (cm^3)	Computed Diameter (mm)	Mass (gm)	Computed Thickness (mm)	Energy E (Joules)	$\bar{R}$	$\bar{P}_{s_1}$	$\bar{t}_{a_1}$	$\bar{T}_{s_1}(+)$	$\bar{I}_{s_1}(+)$	$\bar{T}_s(-)$	$\tilde{I}_s(-)$	$\bar{t}_{a_2}$	$\bar{P}_{s_2}$
4	6.04	540	101	75	1.0	440	2.47	0.028	1.79	1.38	0.025	1.92	0.039	5.13	0.068
							3.08	0.028	2.47	1.24	0.019	1.92	—	5.70	0.053
							3.70	0.021	2.74	1.34	0.016	1.88	0.0260	5.90	0.036
							4.32	0.014	3.48	1.24	0.012	1.84	0.0189	6.53	0.031
5	6.04	501	98.5	76.5	1.1	409	3.95	0.0175	2.64	1.29	0.015	1.84	0.022	5.74	0.025
							4.58	0.0147	3.19	1.46	0.013	1.78	—	6.40	0.019
8	6.04	59	48.3	10.4	0.6	46	2.30	0.032	1.80	1.40	0.029	—	—	—	—
							3.61	0.023	3.07	1.45	0.022	1.93	0.038	6.40	0.0330
							4.92	0.014	4.39	1.40	0.013	1.84	0.021	7.59	0.0207
							6.24	0.013	5.92	1.32	0.012	1.89	0.017	8.99	0.0160
							7.55	0.0099	6.84	1.22	0.0086	1.84	0.012	9.83	0.0113
							8.86	0.0074	7.98	1.32	0.0065	1.89	0.0082	11.10	0.00680
9	6.11	73	51.9	7.8	0.4	52	2.20	0.048	1.17	1.30	0.037	—	—	—	—
							3.45	0.039	2.93	1.26	0.029	1.93	0.055	6.03	0.0574
							4.70	0.023	4.06	1.17	0.017	1.76	0.030	6.91	0.0408
							5.96	0.019	5.45	1.17	0.016	1.80	0.017	8.30	0.0288
							7.21	0.016	6.33	1.17	0.011	1.68	0.016	9.18	0.0223
							8.47	0.012	7.54	1.13	0.0085	1.80	0.013	10.56	0.0156

Freon-12 Vapor Bursting Sphere Data

Test No.	Internal Pressure (p_1/p_a)	Volume (cm^3)	Computed Diameter (mm)	Mass (gm)	Computed Thickness (mm)	Energy E (Joules)	$\bar{R}$	$\bar{P}_{s_1}$	$\bar{t}_{a_1}$	$\bar{T}_{s_1}(+)$	$\bar{I}_{s_1}(+)$	$\bar{T}_s(-)$	$\bar{I}_s(-)$	$\bar{t}_{a_2}$	$\bar{P}_{s_2}$
16	5.90	77	52.8	7.0	0.3	62	1.63	0.065	0.748	1.07	0.0457	1.82	0.0756	3.74	0.114
							2.07	0.057	1.42	1.35	0.0435	1.90	0.0648	3.66	0.0665
							3.26	0.036	2.48	1.23	0.0265	1.70	0.0463	5.42	0.0484
							4.44	0.022	3.61	1.15	0.0147	1.74	0.0267	6.49	0.0304
							5.63	0.020	4.83	1.15	0.0130	1.78	0.0210	7.87	0.0195
							6.81	0.015	5.70	1.07	0.00980	1.78	0.0152	7.91	0.0172
							8.00	0.011	6.84	1.19	0.00787	1.70	0.0116	9.73	0.0126
							9.33	0.011	8.19	1.23	0.00814	1.82	0.0127	11.24	0.0134
17	6.04	83	54.1	8.2	0.4	66	1.60	0.069	1.04	1.20	0.0513	1.82	0.0798	4.03	0.100
							2.03	0.049	1.11	1.40	0.0383	1.78	0.0627	5.43	0.0608
							3.19	0.034	2.59	1.20	0.0259	1.74	0.0508	6.71	0.0406
							4.35	0.021	3.75	1.16	0.0165	1.67	0.0296	6.60	0.0219
							5.51	0.018	4.92	1.12	0.0128	1.82	0.0210	7.95	0.0177
							6.68	0.013	5.86	1.12	0.00931	1.74	0.0156	8.72	0.0119
							7.84	0.011	6.94	1.24	0.00804	1.86	0.0121	10.04	0.00952
							9.14	0.012	8.30	1.16	0.00847	1.90	0.0135	11.44	0.0134
18	5.90	541	101.1	100.5	1.3	441	1.00	0.069	--	1.44	0.0572	1.96	0.105	3.40	0.101
							1.23	0.055	0.515	1.54	0.0451	1.96	0.0818	4.02	0.0937
							1.85	0.041	0.844	1.36	0.0333	1.96	0.0662	4.16	0.0709
							2.47	0.027	1.48	1.34	0.0206	1.92	0.0381	4.76	0.0454
							3.08	0.022	2.08	1.36	0.0189	2.00	0.0310	5.44	0.0366
							3.70	0.018	2.66	1.26	0.0130	1.96	0.0257	5.89	0.0253
							4.32	0.015	3.32	1.48	0.0138	1.92	0.0190	6.73	0.0200
							5.01	0.015	3.93	1.42	0.0129	1.94	0.0212	7.23	0.0225
19	5.90	527	100.2	94.0	1.3	429	1.01	0.074	--	1.41	0.0612	2.01	0.109	3.43	0.0803
							1.24	0.064	0.415	1.50	0.0516	1.93	0.0710	3.84	0.0849
							1.87	0.043	0.685	1.31	0.0365	1.95	0.0653	3.97	0.0840
							2.49	0.027	1.35	1.31	0.0218	1.89	0.0384	4.55	0.0387
							3.11	0.023	2.10	1.31	0.0195	1.97	0.0276	5.30	0.0336
							3.73	0.019	2.53	1.35	0.0169	1.91	0.0241	5.82	0.0242
							4.35	0.015	3.09	1.43	0.0135	2.01	0.0186	6.54	0.0183
							5.05	0.015	3.84	1.43	0.0129	1.93	0.0191	7.71	0.0192

39

Table B-2 (Cont'd.)

Freon-12 Vapor Bursting Sphere Data

Test No.	Internal Pressure (p_1/p_a)	Volume (cm^3)	Computed Diameter (mm)	Mass (gm)	Computed Thickness (mm)	Energy E (Joules)	$\bar{R}$	$\bar{p}_{s_1}$	$\bar{t}_{a_1}$	$\bar{T}_{s_1}(+)$	$\bar{I}_{s_1}(+)$	$\bar{T}_s(-)$	$\bar{I}_s(-)$	$\bar{t}_{a_2}$	$\bar{p}_{s_2}$
20	3.45	568	102.7	50.5	0.7	203	1.30	0.048	--	1.52	0.0457	2.13	0.0834	4.45	0.0658
							1.60	0.040	0.56	1.84	0.0399	2.00	0.0616	4.45	0.0525
							2.39	0.031	1.09	1.63	0.0300	2.05	0.0560	4.80	0.0465
							3.19	0.019	1.95	1.47	0.0171	2.08	0.0319	5.52	0.0277
							3.99	0.015	2.72	1.63	0.0145	2.05	0.0250	6.42	0.0216
							4.79	0.013	3.28	1.68	0.0123	1.95	0.0178	6.90	0.0171
							5.58	0.0098	4.00	1.63	0.00926	2.05	0.0138	7.73	0.0121
							6.48	0.0098	5.04	1.57	0.00926	2.05	0.0147	8.61	0.0146
21	3.45	616	105.5	68.3	0.8	226	1.25	0.040	0.412	1.72	0.0409	2.01	0.0591	4.14	0.0648
							1.54	0.033	0.944	1.80	0.0355	2.14	0.0567	4.86	0.0443
							2.31	0.025	1.30	1.60	0.0258	2.06	0.0497	4.97	0.0361
							3.08	0.015	2.01	1.54	0.0151	2.08	0.0281	5.74	0.0207
							3.85	0.014	2.80	1.67	0.0133	2.03	0.0213	6.43	0.0168
							4.62	0.011	3.40	1.67	0.0105	1.96	0.0151	7.02	0.0128
							5.39	0.0084	4.30	1.72	0.00834	2.03	0.0123	8.10	0.00882
							6.26	0.0084	4.91	1.67	0.00901	2.03	0.0138	9.44	0.0130

REFERENCES

1. E. D. Esparza and W. E. Baker, "Measurement of Blast Waves From Bursting Pressurized Frangible Spheres," NASA CR-2843, 1977.

2. D. W. Boyer, H. L. Brode, I. I. Glass, and J. G. Hall, "Blast from a Pressurized Sphere," UTIA Report No. 48, University of Toronto, Canada, January 1958.

3. W. E. Baker, Explosions in Air, University of Texas Press, Austin, TX, 1973.

4. S. L. Huang and P. C. Chou, "Calculations of Expanding Shock Waves and Late-Stage Equivalence," Drexel Institute of Technology Report No. 125-12, April 1968.

5. R. A. Strehlow and W. E. Baker, "The Characterization and Evaluation of Accidental Explosions," Progress in Energy and Combustion Science, Vol. 2, No. 1, pp 27-60, 1976.

6. B. Maurer, H. Schneider, K. Hess, and W. Leuckel, "Modelling of Vapor Cloud Dispersion and Deflagration After Bursting of Tanks Filled with Liquified Gas" (Translation by R. A. Mayer), Enlarged Version of Lecture before International Seminar: ELCALAP for Structural Safeguards and Containment Structures, Berlin, West Germany, September 1975.

7. ASHRAE Handbook of Fundamentals, Am. Soc. of Heating, Refrigerating and Air Conditioning Engineers, Inc., N.Y., 1972.

1. Report No. NASA CR-2811	2. Government Accession No.	3. Recipient's Catalog No.
4. Title and Subtitle MEASUREMENTS OF BLAST WAVES FROM BURSTING FRANGIBLE SPHERES PRESSURIZED WITH FLASH-EVAPORATING VAPOR OR LIQUID		5. Report Date November 1977
		6. Performing Organization Code
7. Author(s) E. D. Esparza and W. E. Baker		8. Performing Organization Report No. SwRI 02-4599
		10. Work Unit No.
9. Performing Organization Name and Address Southwest Research Institute P. O. Drawer 28510 San Antonio, Texas 78284		11. Contract or Grant No. NSG-3008
		13. Type of Report and Period Covered Contractor Report
12. Sponsoring Agency Name and Address National Aeronautics and Space Administration Washington, D.C. 20546		14. Sponsoring Agency Code

15. Supplementary Notes

Final report. Project Manager, Paul M. Ordin, Space Propulsion and Power Division, NASA Lewis Research Center, Cleveland, Ohio 44135

16. Abstract

Laboratory experiments were conducted to obtain incident overpressure data from frangible spheres pressurized with a flash-evaporating fluid in liquid and vapor form. Glass spheres under higher than ambient internal pressure of Freon-12 were purposely burst to obtain time histories of overpressure. Non-dimensional peak pressures, arrival and duration times, and impulses are presented, and whenever possible plotted and compared with compiled data for Pentolite high-explosive. The data are generally quite repeatable and show differences from blast data produced by condensed high-explosives.

17. Key Words (Suggested by Author(s)) Blast waves; Non-ideal explosions; Blast pressures; Blast impulses; Bursting frangible pressure vessels; Flash-evaporating liquids; Vapor explosions	18. Distribution Statement Unclassified - unlimited STAR Category 28		
19. Security Classif. (of this report) Unclassified	20. Security Classif. (of this page) Unclassified	21. No. of Pages 44	22. Price* A03